

Logical stochastic resonance in a cross-bifurcation non-smooth system

Yuqing Zhang(张宇青) and Youming Lei(雷佑铭)
Citation: Chin. Phys. B, 2024, 33 (**3**): 038201. DOI: 10.1088/1674-1056/acf11e
Journal homepage: http://cpb.iphy.ac.cn; http://iopscience.iop.org/cpb

What follows is a list of articles you may be interested in

Novel two-directional grid multi-scroll chaotic attractors based on the Jerk system

Peng-Fei Ding(丁鹏飞), Xiao-Yi Feng(冯晓毅)†, and Cheng-Mao Wu(吴成茂)
Chin. Phys. B, 2020, 29 (**10**): 108202. DOI: 10.1088/1674-1056/ab9dea

A novel multi-scroll chaotic generator: Analysis, simulation, and implementation

Gui-Tao Zhang(张桂韬), Fa-Qiang Wang(王发强)
Chin. Phys. B, 2018, 27 (**1**): 018201. DOI: 10.1088/1674-1056/27/1/018201

Bursting oscillations in a hydro-turbine governing system with two time scales

Qing-Shuang Han(韩青爽), Di-Yi Chen(陈帝伊), Hao Zhang(张浩)
Chin. Phys. B, 2017, 26 (**12**): 128202. DOI: 10.1088/1674-1056/26/12/128202

Coexisting hidden attractors in a 4D segmented disc dynamo with one stable equilibrium or a line equilibrium

Jianghong Bao(鲍江宏), Dandan Chen(陈丹丹)
Chin. Phys. B, 2017, 26 (**8**): 080201. DOI: 10.1088/1674-1056/26/8/080201

Nonlinear dynamic characteristics and optimal control of a giant magnetostrictive film-shaped memory alloy composite plate subjected to in-plane stochastic excitation

Zhu Zhi-Wen (竺致文), Zhang Qing-Xin (张庆昕), Xu Jia (许佳)
Chin. Phys. B, 2014, 23 (**8**): 088201. DOI: 10.1088/1674-1056/23/8/088201

Logical stochastic resonance in a cross-bifurcation non-smooth system

Yuqing Zhang(张宇青)[1] and Youming Lei(雷佑铭)[1,2,†]

[1] *School of Mathematics and Statistics, Northwestern Polytechnical University, Xi'an* 710072, *China*
[2] *Ministry of Industry and Information Technology Key Laboratory of Dynamics and Control of Complex Systems, Northwestern Polytechnical University, Xi'an* 710072, *China*

(Received 9 June 2023; revised manuscript received 8 August 2023; accepted manuscript online 17 August 2023)

This paper investigates logical stochastic resonance (LSR) in a cross-bifurcation non-smooth system driven by Gaussian colored noise. In this system, a bifurcation parameter triggers a transition between monostability, bistability and tristability. By using Novikov's theorem and the unified colored noise approximation method, the approximate Fokker–Planck equation is obtained. Then we derive the generalized potential function and the transition rates to analyze the LSR phenomenon using numerical simulations. We simulate the logic operation of the system in the bistable and tristable regions respectively. We assess the impact of Gaussian colored noise on the LSR and discover that the reliability of the logic response depends on the noise strength and the bifurcation parameter. Furthermore, it is found that the bistable region has a more extensive parameter range to produce reliable logic operation compared with the tristable region, since the tristable region is more sensitive to noise than the bistable one.

Keywords: logical stochastic resonance, bifurcation, mean first passage time

PACS: 82.40.Bj, 05.10.Gg, 87.10.Rt **DOI:** 10.1088/1674-1056/acf11e

1. Introduction

In practice, many physical systems are connected to noise. Intuitively it was thought that noise always plays a destructive role. However, with the development of stochastic dynamics it has been discovered that noise can produce unexpectedly ordered behavior in nonlinear dynamical systems. An example of such a phenomenon is stochastic resonance (SR), initially suggested by Benzi *et al.*[1] and Nicolis.[2] Under certain conditions (the combination of external periodic forces, noise and the nonlinearity of the system), an appropriate noise input maximizes the response of the nonlinear system to a weakly periodic signal, giving rise to a 'resonance' phenomenon. SR has been applied to many fields, including weak signal detection,[3] image processing,[4] biological systems,[5,6] energy harvesting,[7,8] neural networks,[9–11] mechanical fault diagnosis,[12,13] etc.

Logical stochastic resonance (LSR) provides a completely new method for building reliable logic gates, which was initially suggested by Murali *et al.*[14] Research has revealed that when two square waves act as input signals, a bistable system can generate a logic output under optimal noise. Moreover, as the noise increases, the success probability of the system response first rises and then falls. Then the LSR phenomenon was confirmed in an electronic circuit model.[15] Inspired by this pioneering study, numerous earlier publications concentrated on the separate study of LSR in bistable or tristable systems. For instance, Gaussian colored noise[16] and non-Gaussian noise,[17] such as sine-Wiener noise,[18] Lévy noise.[19] and α-stable noise,[20] have been shown to produce logic operations in bistable systems. In addition, it has been demonstrated that correlated internal and external noises[21–23] can also produce logic operations in bistable systems. It has also been shown that other elements can produce logic operations in bistable systems, including system parameters,[24] time delay,[25–27] coupling between two subsystems,[28] and periodic and non-periodic forces.[29–31] Since three different inputs correspond to two outputs in a bistable system this may cause information to be lost, making XOR logic unattainable. Storni *et al.*[32] expanded upon the existing research in bistable systems and applied it to a tristable system, consequently resulting in the attainment of XOR logic. Subsequently Zhang *et al.*[33,34] researched the LSR phenomenon of a tristable system driven by Gaussian colored noise and non-Gaussian noise, and confirmed the LSR phenomenon in analog circuits; however, for bistable and multistable systems which is better suited to produce reliable logic operations? Lu *et al.*[35] investigated the LSR performance of a tristable system and traditional bistable system. Liao *et al.*[36] compared the LSR performance of a proposed quadstable system and tristable system as reconfigurable logic gates. Previous studies had considered two different systems: for the same system with bistable and tristable regions, which is more suitable for generating logic operations? Therefore, we can consider a cross-bifurcation non-smooth system with a bifurcation parameter resulting in an alteration in monostability, bistability and tristability.

[†]Corresponding author. E-mail: leiyouming@nwpu.edu.cn

© 2024 Chinese Physical Society and IOP Publishing Ltd

Since it is common for a nonlinear system to bifurcate from a bistable state to a multistable one due to friction and collision, study of stochastic resonance in a bifurcation system is unavoidable. Kang *et al.*[37] studied a single-mode nonlinear optical system and demonstrated that the dependence of the relaxation rate on the noise intensity in monostable and multistable cases exhibited a large difference. It is well known that the changing of parameters in nonlinear systems can cause bifurcation cascades, in which existing branches of states are eliminated and new states emerge. Nicolis and Nicolis[38] considered a nonlinear stochastic dynamical system with a bifurcation parameter across monostable, bistable and multistable regimes. They came up with analytical equations for the response and optimal responding conditions for the bifurcation parameter, the noise amplitude and the frequency of external excitation based on response theory. Lei and colleagues[39,40] studied a non-smooth system with a controllable parameter that bifurcates as the controllable parameter changes. They discussed the SR phenomenon in bistable and multistable areas. It was demonstrated that the multistability of the system improves the optimal transition rate and the optimal response amplitude of the system.

In this work, we consider a cross-bifurcation non-smooth system with a bifurcation parameter that transits from tristable to bistable regions as the bifurcation parameter changes. Therefore, we focus on the effect of the bifurcation parameter on the LSR in different regions. In Section 2, we describe the cross-bifurcation non-smooth system under Gaussian colored noise excitation. In Section 3, we conduct a bifurcation analysis for this system and derive expressions for the generalized potential function and the mean first passage time (MFPT) in the bistable and tristable regions, respectively. The success probability is introduced to measure the reliability of logic response, and the difference in LSR in bistable and tristable areas is discussed. The conclusions are drawn in Section 4.

2. Cross-bifurcation non-smooth system and measurement of LSR

In this section we consider a cross-bifurcation non-smooth system under Gaussian colored noise excitation. The Langevin equation of the system has the following form:

$$\dot{x} = f(x) + I(t) + \xi(t), \tag{1}$$

where $f(x) = x - x^3 + r\mathrm{sgn}(x)$ and r is the controllable parameter that causes the system to bifurcate, $I(t)$ is a low-amplitude signal and $\xi(t)$ is a Gaussian colored noise with statistical properties

$$\langle \xi(t) \rangle = 0, \quad \langle \xi(t)\xi(t') \rangle = \frac{D}{\tau} \exp\left(-\frac{|t-t'|}{\tau} \right), \tag{2}$$

where D is the noise strength and τ is the correlation time.

Using N inputs to generate N square waves, a logical correspondence between inputs and outputs can be established. Specifically, I is a low-amplitude input, $I = I_1 + I_2$, where I_1 and I_2 encode the two logic inputs. We drive the cross-bifurcation non-smooth system with the signal I. The logic inputs can be 0 or 1, so there are four different logic input sets (I_1, I_2): $(0,0)$, $(1,0)$, $(0,1)$ and $(1,1)$. The signal $I_{1,2}$ has a value of $-K$ for a logical 0, whereas it takes on a value of K for a logical 1. Since the input sets $(0,1)$ and $(1,0)$ produce the same I, the four different input conditions (I_1, I_2) produce three different I values: $-2K$, 0, $2K$. As a result, the input signal I is a three-level aperiodic waveform.

3. Logical stochastic resonance under colored noise

The potential function corresponding to Eq. (1) takes the form

$$U(x) = \begin{cases} -\dfrac{1}{2}x^2 + \dfrac{1}{4}x^4 - rx, & x > 0, \\ -\dfrac{1}{2}x^2 + \dfrac{1}{4}x^4 + rx, & x \le 0. \end{cases} \tag{3}$$

It can be found that the potential function has a point where the first-order derivative is discontinuous

$$x_3 = 0, \tag{4}$$

and has four extreme points

$$\begin{aligned} x_1 = -x_5 &= -\frac{2\sqrt{3}}{3}\cos\left[\frac{1}{3}\arccos\left(-\frac{3\sqrt{3}}{2}r\right) - \frac{\pi}{3}\right], \\ x_2 = -x_4 &= -\frac{2\sqrt{3}}{3}\cos\left[\frac{1}{3}\arccos\left(-\frac{3\sqrt{3}}{2}r\right) + \frac{\pi}{3}\right]. \end{aligned} \tag{5}$$

It can be found that when $r = -2\sqrt{3}/9$, x_1 and x_2 merge and x_4 and x_5 merge. When $r < -2\sqrt{3}/9$, the system has only one stable point x_3. In the region $-2\sqrt{3}/9 < r < 0$, the system has three stable points x_1, x_3 and x_5, and two unstable points x_2 and x_4. When $r = 0$, x_2 and x_4 merge and disappear, and x_3 becomes unstable. In the region $r > 0$, the system has two stable points x_1 and x_5 and one unstable point x_3. Figure 1 displays the corresponding bifurcation diagram. At $r = -2\sqrt{3}/9$, the system has two saddle-node bifurcations making the system change from monostable to tristable. As the logic outputs have two values, it is difficult for a monostable system to generate the LSR phenomenon, therefore this bifurcation point is not studied. At $r = 0$, the system has a subcritical pitchfork bifurcation making the system change from tristable to bistable. Earlier publications have concentrated on the separate study of LSR in bistable or tristable systems. Now we consider the bistable and tristable cases uniformly in this work. In the following we shall investigate LSR in bistable and tristable areas respectively.

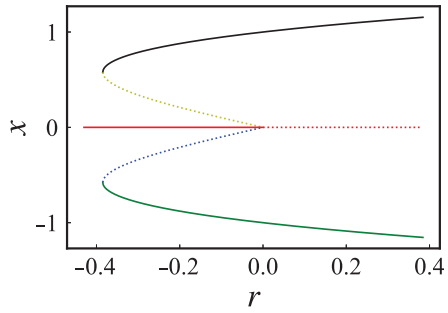


Fig. 1. Bifurcation diagram of system (1) on the bifurcation parameter r. At $r=-2\sqrt{3}/9$, the system has two saddle-node bifurcations making the system change from monostable to tristable. At $r=0$, the system has a subcritical pitchfork bifurcation making the system change from tristable to bistable.

3.1. Bistability

In the bistable region, the system has two symmetrical potential wells, but there are three different logical inputs. This results in a memorable output value when the logical input is 0. In other words, the output value is determined by the output value of the previous state. Specifically, if the previous output is -1, then the current output will also be -1, and if the previous output is 1, then the current output will be 1. Therefore, with reference to Table 1 we find that the logic response of the system cannot realize a reliable logic operation, for which a bias parameter is added to deflect the potential. Thus, the Langevin equation is rewritten as

$$\dot{x}=f(x)+I(t)+\xi(t), \tag{6}$$

where $f(x)=x-x^3+r\mathrm{sgn}(x)+G$ and G is a bias parameter.

As shown in Fig. 2, the tilt of the potential function is determined by the bias parameter G. When $G>0$, the bistable potential function tilts to the right, as shown by the red dashed line in the figure. When the logic input is 0, the particle will be in the well at x_+. With reference to Table 1 we find that in this case the system can implement an OR/NOR logic operation. When $G<0$, the bistable potential function tilts to the left, as shown by the green dotted line in the figure. When the logic input is 0, the particle will be in the well at x_-. With reference to Table 1 this reveals that the system can implement AND/NAND logic operations.

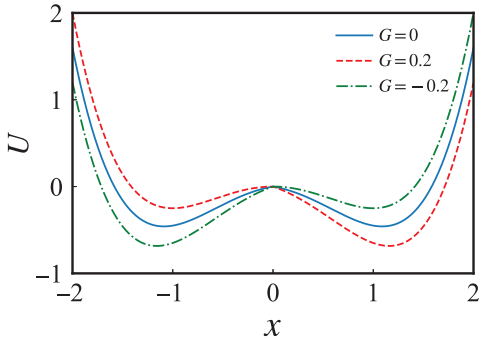


Fig. 2. Potential well for various G values. The blue line denotes the symmetric bistable well, the green line denotes the AND/NAND logic operation and the red line denotes the OR/NOR logic operation.

Table 1. For the four logic operations, the connection between the four input sets and the outputs.

Input set	OR	AND	NOR	NAND
(0,0)	0	0	1	1
(0,1)/(1,0)	1	0	0	1
(1,1)	1	1	0	0

The logical output of the system is decided by its state. For example, if its state is in one well, the output can be considered as a logical 1, and if it is in another well, the output can be considered as a logical 0. Specifically for a bistable system with two potential wells at x_+ and x_-, the logical output of the system is considered to be 1 when its state is in right well (x_+) and it is considered to be 0 when its state is in left well (x_-). The output is thus 'toggled' when the system switches wells. According to Table 1 the system can implement the required types of logic gates.

The potential function corresponding to Eq. (6) takes the form

$$U(x)=-\frac{1}{2}x^2+\frac{1}{4}x^4-rx\mathrm{sgn}(x)-Gx. \tag{7}$$

Using Novikov's theorem and the unified colored noise approximation method,[41–43] the approximate Fokker–Planck equation corresponding to Eq. (6) is written as

$$\frac{\partial P(x)}{\partial t}=-\frac{\partial}{\partial x}\left[f(x)P(x)\right]+\frac{\partial^2}{\partial x^2}\left[B(x)P(x)\right], \tag{8}$$

where $B(x)=\dfrac{D}{1-\tau f'(x_\mathrm{s})}$, $x_\mathrm{s}=\begin{cases}x_1, & x\le 0,\\ x_5, & x>0.\end{cases}$

In the adiabatic limit, the stationary probability density (SPD) is obtained as

$$P_\mathrm{s}=N\exp\left[-U_\mathrm{g}(x)\right], \tag{9}$$

where N is a normalization constant and the generalized potential function U_g is given as

$$U_\mathrm{g}(x)=\frac{1-\tau f'(x_\mathrm{s})}{D}\left[-\frac{1}{2}x^2+\frac{1}{4}x^4-rx\mathrm{sgn}(x)-Gx\right]. \tag{10}$$

In the bistable region, the mean first passage time is derived from

$$\begin{aligned}T_{15}(x_1\to x_5)&=\int_{x_1}^{x_5}\frac{\mathrm{d}x}{\psi(x)}\int_{-\infty}^{x}\frac{\psi(y)}{B(y)}\mathrm{d}y,\\ T_{51}(x_5\to x_1)&=\int_{x_1}^{x_5}\frac{\mathrm{d}x}{\psi(x)}\int_{x}^{+\infty}\frac{\psi(y)}{B(y)}\mathrm{d}y,\end{aligned} \tag{11}$$

where

$$\psi(x)=\exp[-U_\mathrm{g}(x)]. \tag{12}$$

In the bistable region, point x_3 is unstable when the system is non-smooth so the Gaussian approximation cannot be used. Thus, the steepest-descent approximation allows us to estimate the following:

$$\int_{-\infty}^{x}\frac{\psi(y)}{B(y)}\mathrm{d}y$$

$$\approx \frac{1-\tau f'(x_1)}{D}\int_{-\infty}^{+\infty}\exp\left[-U_{\rm g}(x_1,t)+\frac{1}{2}U''_{\rm g}(x_1)(y-x_1)^2\right]{\rm d}y$$
$$= \exp[-U_{\rm g}(x_1)]\frac{\sqrt{2\pi}}{\sqrt{U''_{\rm g}(x_1)}}\frac{1-\tau f'(x_1)}{D}. \quad (13)$$

For $\int_{x_1}^{x_5}\frac{1}{\psi(x)}{\rm d}x$, expanding $U_{\rm g}(x,t)$ in the left and right neighborhoods of $x=x_3$, we can obtain

$$\begin{aligned}&\int_{x_1}^{x_5}\frac{1}{\psi(x)}{\rm d}x\\ &\approx \int_{-\infty}^{x_3}\exp\left[U_{\rm g}(x_3,t)+U'_{\rm g-}(x_3)(x-x_3)\right]{\rm d}x\\ &\quad+\int_{x_3}^{+\infty}\exp\left[U_{\rm g}(x_3,t)+U'_{\rm g+}(x_3)(x-x_3)\right]{\rm d}x\\ &= \exp\left[U_{\rm g}(x_3)\right]\left(\frac{1}{U'_{\rm g-}(x_3)}-\frac{1}{U'_{\rm g+}(x_3)}\right). \quad (14)\end{aligned}$$

Hence, the analytical expression for the MFPT takes the form

$$\begin{aligned}&T_{15}(x_1\to x_5)\\ &= \exp\left[U_{\rm g}(x_3)-U_{\rm g}(x_1)\right]\frac{\sqrt{2\pi}(1-\tau f'(x_1))}{D\sqrt{U''_{\rm g}(x_1)}}\\ &\quad\times\left(\frac{1}{U'_{\rm g-}(x_3)}-\frac{1}{U'_{\rm g+}(x_3)}\right), \quad (15)\end{aligned}$$

similarly

$$\begin{aligned}&T_{51}(x_5\to x_1)\\ &= \exp\left[U_{\rm g}(x_3)-U_{\rm g}(x_5)\right]\frac{\sqrt{2\pi}(1-\tau f'(x_5))}{D\sqrt{U''_{\rm g}(x_5)}}\\ &\quad\times\left(\frac{1}{U'_{\rm g-}(x_3)}-\frac{1}{U'_{\rm g+}(x_3)}\right). \quad (16)\end{aligned}$$

Therefore, the transition rates are given by

$$\begin{aligned}k_{15} &= \frac{1}{T_{15}} = \exp\left[U_{\rm g}(x_1)\right]\frac{D\sqrt{U''_{\rm g}(x_1)}}{\sqrt{2\pi}(1-\tau f'(x_1))}\\ &\quad\times\left(\frac{U'_{\rm g+}(x_3)U'_{\rm g-}(x_3)}{U'_{\rm g+}(x_3)-U'_{\rm g-}(x_3)}\right),\\ k_{51} &= \frac{1}{T_{51}} = \exp\left[U_{\rm g}(x_5)\right]\frac{D\sqrt{U''_{\rm g}(x_5)}}{\sqrt{2\pi}(1-\tau f'(x_5))}\\ &\quad\times\left(\frac{U'_{\rm g+}(x_3)U'_{\rm g-}(x_3)}{U'_{\rm g+}(x_3)-U'_{\rm g-}(x_3)}\right). \quad (17)\end{aligned}$$

Likewise, when $I=-0.8$, the approximate Fokker–Planck equation is described as

$$\frac{\partial P(x)}{\partial t} = -\frac{\partial}{\partial x}\left[(f(x)-0.8)P(x)\right]+\frac{\partial^2}{\partial x^2}\left[B(x)P(x)\right], \quad (18)$$

where $B(x)=\dfrac{D}{1-\tau f'(x_{\rm s})}$, $x_{\rm s}=\begin{cases}x_1, & x\le 0,\\ x_5, & x>0.\end{cases}$

In the adiabatic limit, the SPD of the system is obtained as

$$P_{\rm s} = N\exp\left[-U_{\rm g}(x)\right], \quad (19)$$

where N is a normalization constant and the generalized potential function $U_{\rm g}$ has the following form:

$$\begin{aligned}U_{\rm g}(x) &= \frac{1-\tau f'(x_{\rm s})}{D}\\ &\quad\times\left[-\frac{1}{2}x^2+\frac{1}{4}x^4-rx{\rm sgn}(x)-Gx+0.8x\right]. \quad (20)\end{aligned}$$

Similarly, the transition rates can be given by

$$\begin{aligned}k_{15} &= \frac{1}{T_{15}} = \exp\left[U_{\rm g}(x_1)\right]\frac{D\sqrt{U''_{\rm g}(x_1)}}{\sqrt{2\pi}(1-\tau f'(x_1))}\\ &\quad\times\left(\frac{U'_{\rm g+}(x_3)U'_{\rm g-}(x_3)}{U'_{\rm g+}(x_3)-U'_{\rm g-}(x_3)}\right),\\ k_{51} &= \frac{1}{T_{51}} = \exp\left[U_{\rm g}(x_5)\right]\frac{D\sqrt{U''_{\rm g}(x_5)}}{\sqrt{2\pi}(1-\tau f'(x_5))}\\ &\quad\times\left(\frac{U'_{\rm g+}(x_3)U'_{\rm g-}(x_3)}{U'_{\rm g+}(x_3)-U'_{\rm g-}(x_3)}\right). \quad (21)\end{aligned}$$

Consider the logic input parameter K to take the value 0.4. Figure 3 displays the response of the system in Eq. (6) at different noise intensities D when the bifurcation parameter $r=0.2$ and the bias parameter $G=0.3$. The red line indicates the logical input and the blue line indicates the output of the system. It can be found that for very weak noise ($D=0.01$) at some moments the state of the particle depends on the previous state at times, for example [8000, 8500], [10000, 12000]. The particle cannot produce a transition and does not move to the desired potential well. For optimal noise ($D=0.2$), the particle is located in the left well when the input is -0.8, and the particle is located in the right well when the input is 0 or 0.8. According to Table 1, if state $x<0$ is interpreted as logical output 0 and state $x>0$ as logical output 1, the system produces a stable OR logic behavior, whereas if state $x>0$ is interpreted as logical output 0 and state $x<0$ as logical output 1, the system produces a stable NOR logic behavior. In the same way, by setting the bias parameter at $G=-0.3$, we can achieve clean AND/NAND gates at an optimal noise intensity. With the enhancement of noise ($D=0.5$), due to frequent transitions of particles, the system gradually produces the wrong logic outputs. Thus, noise-induced logic operation becomes unreliable and the LSR phenomenon is destroyed.

In order to measure the reliability of noise-induced logic operation, we introduce the concept of success probability. The success probability P is expressed as

$$P = \frac{S}{N}, \quad (22)$$

where N is the overall number of runs and S is the number of correct logic outputs. When P approximates to 1, the system generates a reliable logic operation. Using computer simulations to generate sets of logic inputs and continuously inputting different combinations of logic inputs to the system,

the success probability can be obtained. The logic input has four possible input sets $(I_1, I_2) : (0,0), (0,1), (1,0)$ and $(1,1)$. Each run is a random permutation of all the above sets, where each signal input set drives the system for a period of time with time step $\Delta t = 0.01$ s and 1000 s. Then the obtained output is compared with the desired logic output to obtain the correct probability of this set. When this correct probability is above a certain threshold, the set of logic outputs is considered correct. A run is deemed successful only when all four logic outputs are correct.

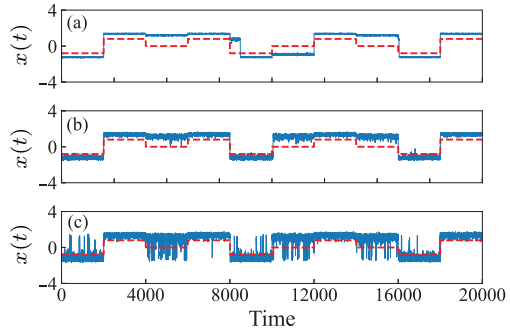


Fig. 3. The logic output $x(t)$ with $r = 0.2$ corresponding to (a) $D = 0.01$, (b) $D = 0.2$, (c) $D = 0.5$. The dashed red line indicates the logical input I, consisting of a combination of I_1 and I_2 which take the value -0.4 when the logic input is 0 and 0.4 when the logic input is 1. Clearly, when $D = 0.2$, we get the desired OR gate.

To further investigate the effect of different parameters on LSR, we plot the variation of P with different parameters in Fig. 4. Figure 4(a) illustrates the variation of P with noise intensity D for fixed parameters $r = 0.2$ and $G = 0.3$. The results show that P increases rapidly with increasing noise strength for weak noise, and then stabilizes to 1. The system appears to have an optimal window of noise strength $(0.100 < D < 0.350)$. The logic response is nearly 100% accurate in an optimal window of the noise, so that the system reliably implements logic operations. As the noise strength continues to increase, the success probability gradually decreases until it tends to 0. The reason for this phenomenon is that the noise strength reflects the amount of energy provided to the particle by the external noise. When the noise strength is small, the energy provided by the noise is too small to support the particle crossing the potential barrier to make the leap between different wells, so that the system cannot produce reliable logic behavior. When the noise strength is too high, the energy provided by the noise is too high, which leads to frequent disorderly transitions between different wells and causes the particle to move in an irregular manner. Therefore, reliable logic behavior cannot be produced. Only when the noise is moderately strong does the energy provided by the noise allow the particle to cross the potential barrier to perform the correct transition behavior between different wells, producing reliable logic behavior.

Further, in Fig. 4(b) we can find how P varies with bifurcation parameter r and noise strength D. In the figure, it can be seen that the system appears to have an optimal window of noise, and the optimal window is related to r. When $r > 0$, the optimal window of noise decreases as r increases and moves to a greater noise strength. Figure 5 depicts the image of the generalized potential function for different values of r, from which it can be found that the height of the potential barrier is affected by r. When $r > 0$, there is a subsequent increase in the potential barrier as r increases. Therefore as r increases, a higher noise intensity is required to enable particle transition. When $I = 0$ the particle can transit to the right well with appropriate noise excitation, as shown in Fig. 5(a), and when $I = -0.8$ the particle can transit to the left well with appropriate noise excitation as depicted in Fig. 5(b). Thus, the optimal window of noise moves to a greater noise strength as r increases. Figure 6 shows that in the bistable region the transition rate decreases as r increases. Thus as r increases, a larger noise intensity is required to make the system produce the LSR phenomenon. This is consistent with the phenomenon that the optimal window of noise moves to a greater noise strength as r increases in Fig. 4(b).

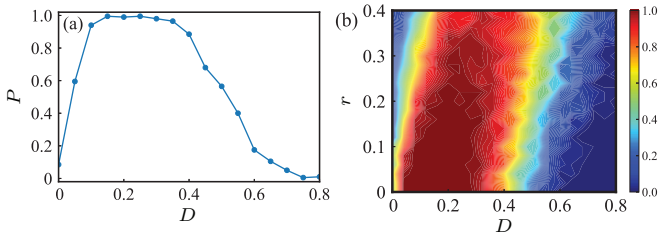


Fig. 4. The variation of success probability P with different parameters in the bistable region: (a) noise intensity D for fixed $r = 0.2$; (b) D and bifurcation parameter r. The system appears to have an optimal window of noise that displays resonance phenomenon with a single flat peak as the noise strength varies. The optimal window of noise decreases as r increases and moves to a greater noise strength.

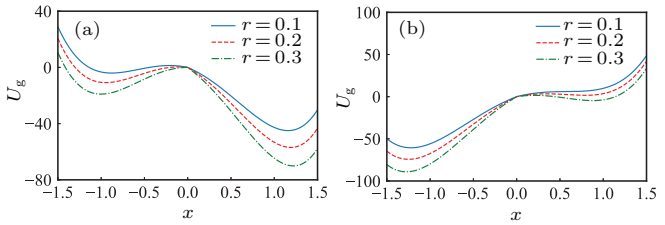


Fig. 5. Generalized potential function at different bifurcation parameters r with $G = 0.3$. (a) When $I = 0$, the particle will be located in the right well under noise excitation. (b) When $I = -0.8$, the particle will be located in the left well under noise excitation. Clearly, the potential barrier increases as r increases.

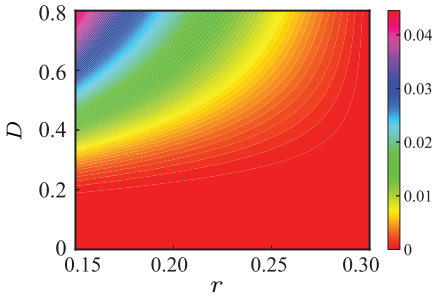


Fig. 6. The variation of transition rate k_{15} with noise intensity D and bifurcation parameter r in the bistable region.

3.2. Tristability

In the tristable region, in addition to the above logic gates, we can also obtain XOR/XNOR logic. We can obtain all the logic behaviors by defining different outputs. According to Table 2, we can set the output to logical 1 if the particle is in the right well and to logical 0 if it is in the others, for which we can obtain the AND logic gate. Likewise, we can obtain the other logic operations by defining the outputs.

Table 2. For the six logic operations, the connection between the four input sets and the outputs.

Logic gate	Left well	Central well	Right well
AND	0	0	1
NAND	1	1	0
OR	0	1	1
NOR	1	0	0
XOR	0	1	0
XNOR	1	0	1

For system (1), according to Novikov's theorem and the unified colored noise approximation method,[41–43] the approximate Fokker–Planck equation is given by

$$\frac{\partial P(x)}{\partial t} = -\frac{\partial}{\partial x}\left[f(x)P(x)\right] + \frac{\partial^2}{\partial x^2}\left[B(x)P(x)\right], \tag{23}$$

where $f(x) = -U'(x)$, $B(x) = \dfrac{D}{1-\tau f'(x_{\rm s})}$, $x_{\rm s} = \begin{cases} x_1, & x \le 0, \\ x_5, & x > 0. \end{cases}$

In the adiabatic limit, the SPD of the system is obtained as

$$P_{\rm s} = N\exp\left[-U_{\rm g}(x)\right], \tag{24}$$

where N is the normalization constant and the generalized potential function $U_{\rm g}$ is written as

$$U_{\rm g}(x) = \frac{1-\tau f'(x_{\rm s})}{D}\left[-\frac{1}{2}x^2 + \frac{1}{4}x^4 - rx{\rm sgn}(x)\right]. \tag{25}$$

In the tristable region, the mean first passage time takes the form

$$\begin{aligned}
T_{13}(x_1 \to x_3) &= \int_{x_1}^{x_3}\frac{{\rm d}x}{\psi(x)}\int_{-\infty}^{x}\frac{\psi(y)}{B(y)}{\rm d}y, \\
T_{31}(x_3 \to x_1) &= \int_{x_1}^{x_3}\frac{{\rm d}x}{\psi(x)}\int_{x}^{x_4}\frac{\psi(y)}{B(y)}{\rm d}y, \\
T_{35}(x_3 \to x_5) &= \int_{x_1}^{x_3}\frac{{\rm d}x}{\psi(x)}\int_{x_2}^{x}\frac{\psi(y)}{B(y)}{\rm d}y, \\
T_{53}(x_5 \to x_3) &= \int_{x_3}^{x_5}\frac{{\rm d}x}{\psi(x)}\int_{x}^{+\infty}\frac{\psi(y)}{B(y)}{\rm d}y,
\end{aligned} \tag{26}$$

where

$$\psi(x) = \exp[-U_{\rm g}(x)]. \tag{27}$$

Similar to the calculation in the bistable region, the expressions for T_{31} and T_{35} can be derived as

$$\begin{aligned}
&T_{31}(x_3 \to x_1) \\
&= \exp\left[U_{\rm g}(x_2) - U_{\rm g}(x_3)\right]\frac{\sqrt{2\pi}(1-\tau f'(x_{\rm s}))}{D\sqrt{U''_{\rm g}(x_2)}} \\
&\quad\times\left(\frac{1}{U'_{\rm g+}(x_3)} - \frac{1}{U'_{\rm g-}(x_3)}\right), \\
&T_{35}(x_3 \to x_5) \\
&= \exp\left[U_{\rm g}(x_4) - U_{\rm g}(x_3)\right]\frac{\sqrt{2\pi}(1-\tau f'(x_{\rm s}))}{D\sqrt{U''_{\rm g}(x_4)}} \\
&\quad\times\left(\frac{1}{U'_{\rm g+}(x_3)} - \frac{1}{U'_{\rm g-}(x_3)}\right).
\end{aligned} \tag{28}$$

Since the point x_3 is not involved in the approximation process for T_{13} and T_{53}, the expression can be obtained by the Gaussian approximation as

$$\begin{aligned}
T_{13}(x_1 \to x_3) &= \exp\left[U_{\rm g}(x_2) - U_{\rm g}(x_1)\right] \\
&\quad\times\frac{2\pi}{\sqrt{U''_{\rm g}(x_1)\left|U''_{\rm g}(x_2)\right|}}\frac{1-\tau f'(x_{\rm s})}{D}, \\
T_{53}(x_5 \to x_3) &= \exp\left[U_{\rm g}(x_4) - U_{\rm g}(x_5)\right] \\
&\quad\times\frac{2\pi}{\sqrt{U''_{\rm g}(x_5)\left|U''_{\rm g}(x_4)\right|}}\frac{1-\tau f'(x_{\rm s})}{D}.
\end{aligned} \tag{29}$$

Considering the mean first passage time of a particle from x_1 to x_5, T_{15} can be obtained from the following expression:

$$T_{15}(x_1 \to x_5) = T_{13}(x_1 \to x_3) + T_{35}(x_3 \to x_5). \tag{30}$$

Similarly, the transition rates can be given by

$$\begin{aligned}
k_{31} &= \frac{1}{T_{31}} = \exp\left[-U_{\rm g}(x_2)\right]\frac{D\sqrt{U''_{\rm g}(x_2)}}{\sqrt{2\pi}(1-\tau f'(x_{\rm s}))} \\
&\quad\times\left(\frac{U'_{\rm g+}(x_3)U'_{\rm g-}(x_3)}{U'_{\rm g-}(x_3) - U'_{\rm g+}(x_3)}\right), \\
k_{35} &= \frac{1}{T_{35}} = \exp\left[-U_{\rm g}(x_4)\right]\frac{D\sqrt{U''_{\rm g}(x_4)}}{\sqrt{2\pi}(1-\tau f'(x_{\rm s}))} \\
&\quad\times\left(\frac{U'_{\rm g+}(x_3)U'_{\rm g-}(x_3)}{U'_{\rm g-}(x_3) - U'_{\rm g+}(x_3)}\right), \\
k_{13} &= \frac{1}{T_{13}} = \exp\left[U_{\rm g}(x_1) - U_{\rm g}(x_2)\right]\frac{D}{1-\tau f'(x_{\rm s})} \\
&\quad\times\frac{\sqrt{U''_{\rm g}(x_1)\left|U''_{\rm g}(x_2)\right|}}{2\pi}, \\
k_{53} &= \frac{1}{T_{53}} = \exp\left[U_{\rm g}(x_5) - U_{\rm g}(x_4)\right]\frac{D}{1-\tau f'(x_{\rm s})} \\
&\quad\times\frac{\sqrt{U''_{\rm g}(x_5)\left|U''_{\rm g}(x_4)\right|}}{2\pi}, \\
k_{15} &= \frac{1}{T_{15}} = \frac{1}{T_{13}+T_{35}}.
\end{aligned} \tag{31}$$

Likewise, when $I = 0.8$, the approximate Fokker–Planck equation is written as

$$\frac{\partial P(x)}{\partial t} = -\frac{\partial}{\partial x}\left[(f(x)+0.8)P(x)\right] + \frac{\partial^2}{\partial x^2}\left[B(x)P(x)\right], \tag{32}$$

where $f(x) = -U'(x)$, $B(x) = \dfrac{D}{1-\tau f'(x_s)}$, $x_s = \begin{cases} x_1, & x \le 0, \\ x_5, & x > 0. \end{cases}$

In the adiabatic limit, the SPD of the system is obtained as

$$P_s = N \exp\left[-U_g(x)\right], \tag{33}$$

where N is the normalization constant and the generalized potential function U_g is given as

$$U_g(x) = \frac{1-\tau f'(x_s)}{D}\left[-\frac{1}{2}x^2 + \frac{1}{4}x^4 - rx\,\mathrm{sgn}(x) - 0.8x\right]. \tag{34}$$

Similarly, the transition rates can be given by

$$\begin{aligned}
k_{31} &= \frac{1}{T_{31}} = \exp\left[-U_g(x_2)\right] \frac{D\sqrt{U_g''(x_2)}}{\sqrt{2\pi}(1-\tau f'(x_s))} \\
&\quad \times \left(\frac{U'_{g+}(x_3)U'_{g-}(x_3)}{U'_{g-}(x_3) - U'_{g+}(x_3)}\right), \\
k_{35} &= \frac{1}{T_{35}} = \exp\left[-U_g(x_4)\right] \frac{D\sqrt{U_g''(x_4)}}{\sqrt{2\pi}(1-\tau f'(x_s))} \\
&\quad \times \left(\frac{U'_{g+}(x_3)U'_{g-}(x_3)}{U'_{g-}(x_3) - U'_{g+}(x_3)}\right), \\
k_{13} &= \frac{1}{T_{13}} = \exp\left[U_g(x_1) - U_g(x_2)\right] \\
&\quad \times \frac{D}{1-\tau f'(x_s)} \frac{\sqrt{U_g''(x_1)\left|U_g''(x_2)\right|}}{2\pi}, \\
k_{53} &= \frac{1}{T_{53}} = \exp\left[U_g(x_5) - U_g(x_4)\right] \\
&\quad \times \frac{D}{1-\tau f'(x_s)} \frac{\sqrt{U_g''(x_5)\left|U_g''(x_4)\right|}}{2\pi}.
\end{aligned} \tag{35}$$

For the case of system (1) in the region $-2\sqrt{3}/9 < r < 0$, we consider the logic input parameter K to take the value 0.4. Figure 7 displays the response of the system in Eq. (1) at different noise intensities D when the bifurcation parameter $r = -0.35$. For very weak noise ($D = 0.003$), at some moments the particle cannot move to the desired well, for example [4000, 5500], [10000, 12000], [14000, 14500]. Therefore, the system cannot generate a reliable logic operation. For optimal noise ($D = 0.015$), the system response yields a reliable logic operation. As the noise continues to increase ($D = 0.1$), the particle transits frequently in the left and right potential wells when the logic input is 0. This LSR phenomenon is destroyed. Comparing with Fig. 3, it can be found that the same phenomenon occurs in the tristable region as in the bistable region, where the presence of optimal noise intensity allows the system to produce reliable logic operations. However, the value of the optimal noise strength in the tristable region is much smaller than that in the bistable region.

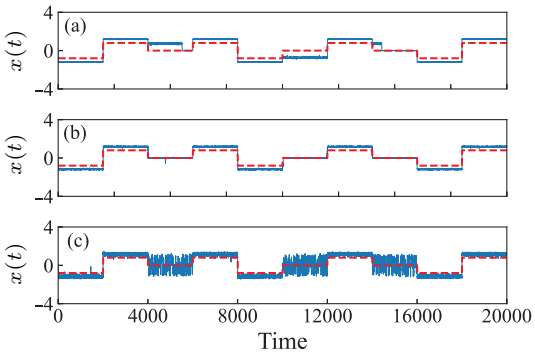


Fig. 7. The logic output $x(t)$ with $r = -0.35$ corresponding to (a) $D = 0.003$, (b) $D = 0.015$, (c) $D = 0.1$. The dashed red line indicates the logic input I, consisting of a combination of I_1 and I_2 which take the value -0.4 when the logic input is 0 and 0.4 when the logic input is 1. Clearly, when $D = 0.015$, we can get the desired logic gate.

Further, Fig. 8 illustrates the variation of the success probability P with different parameters. In Fig. 8(a) we plot the variation of P with noise intensity D for a fixed parameter $r = -0.35$. It is found that P increases rapidly with increasing noise strength for weak noise, and then stabilizes to 1. The system appears to have an optimal window of noise strength ($0.008 < D < 0.026$). In the optimal noise window, the logic response is nearly 100% accurate. The success probability gradually decreases as the noise strength increases, until it tends to 0. Compared with Fig. 4(a), Fig. 8(a) shows that the optimal noise value in the tristable region is much smaller than in the bistable region, and the optimal window interval for noise in the tristable region is also much smaller, indicating that the tristable region is more sensitive to noise.

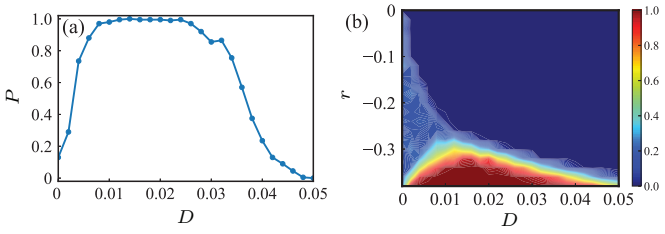


Fig. 8. The variation of success probability P with different parameters in the tristable region: (a) noise intensity D for fixed $r = -0.35$, (b) D and bifurcation parameter r. When $r < -0.33$, the system produces a reliable logic response and the optimal noise interval becomes larger as r decreases.

To further analyze the variation of P with r and D, we plot Fig. 8(b). It is found that the system cannot generate a reliable logic response when $-0.33 < r < 0$. When $r < -0.33$, the system generates a reliable logic response and the optimal noise interval becomes larger as r decreases. Figure 9 depicts the image of the generalized potential function U_g for different values of r. From the figure, it can be found that the height of the potential barrier is influenced by r. This shows that as r increases, there is a subsequent increase in the potential barrier. Therefore, the higher the value of r, the larger the noise intensity required to enable particle transition. However, for some high values of r, the height of the potential barrier is too

large to cause the particle to transit. Thus, it is impossible to generate a correct logic operation. Figure 10 shows that the range of moderate transition rates increases as r decreases in the tristable region, which is consistent with the phenomenon in Fig. 8(b). Comparing with Fig. 4(b), we see that the range of values of r that can produce reliable logic operation in the tristable region is much smaller than in the bistable region, and that both the optimal noise values and the corresponding optimal noise interval range are much smaller. Comparing Figs. 5 and 9, it is found that the potential barrier height in the bistable region is much higher than in the tristable region, so the bistable region needs a higher noise strength to make the particle transition. The potential barriers from the middle well to the two side wells are much smaller in the tristable region than the barriers in the bistable region, so a small noise may cause the particle to make frequent transitions when initiated in the middle well. Therefore, the optimal band of noise in the tristable region is narrower. Comparison of Figs. 6 and 10 reveals that a smaller noise in the tristable region gives a moderate, optimum transition rate. Thus, the tristable region is more sensitive to noise.

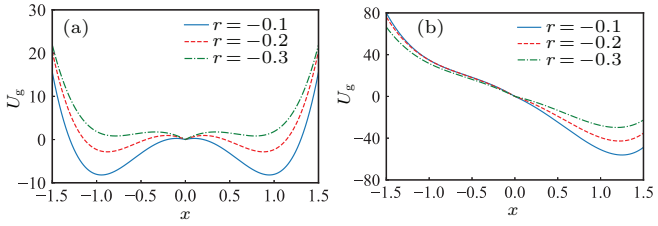


Fig. 9. Generalized potential function at different bifurcation parameters r. (a) When $I=0$, the particle will be located in the middle well under noise excitation. (b) When $I=0.8$, the particle will be located in the right well under noise excitation. Clearly, the potential barrier increases as r increases.

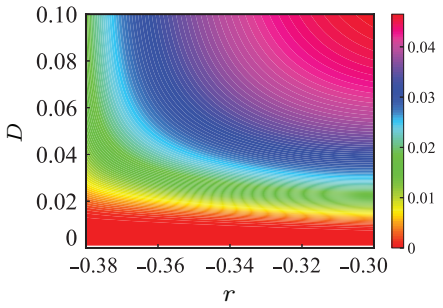


Fig. 10. The variation of transition rate k_{15} with noise intensity D and bifurcation parameter r in the tristable region.

4. Conclusions

In this work, we investigate the logic operation of a cross-bifurcation non-smooth system with bistable and tristable regions. By using Novikov's theorem and the unified colored noise approximation method, we obtain the approximate Fokker–Planck equation and the generalized potential function to analyze the LSR phenomenon with numerical simulations. We numerically simulate the system's logic operation in the bistable and tristable regions and perform a comparative analysis for the two regions. We show that the tristable region is more sensitive to noise than the bistable region. The optimal noise value in the tristable region is much smaller than that in the bistable region. Furthermore, the range of bifurcation parameters that can produce reliable logic output in the tristable region is much smaller, and the optimal noise strength range is smaller than in the bistable region. Similar results can be supported through the analysis of the generalized potential function and transition rate. We show in this work that tristability significantly enhances the transition rate. For example, this phenomenon is similar to the two-step nucleation mechanism in the crystallization of the protein lysozyme, where the intermediate stable state of proteins was found experimentally to accelerate the crystallization rate since tristability in two-step nucleation improves the transition rate and provides a powerful method of controlling the nucleation process. Similarly, the LSR mechanism in tristable dynamics is more sensitive than in bistable dynamics in the over-damped non-smooth system and can be utilized to implement more reliable logic gates in resonant tunneling diodes and simple circuits, and in monitoring weak targets in water degradation images and so on. Our results can be applied to relative experiments and help in selecting optimum parameters for actual implementations.

Acknowledgements

Project supported by the National Natural Science Foundation of China (Grant No. 12072262) and the Shaanxi Computer Society & Xiangteng Company Foundation.

References

[1] Benzi R, Sutera A and Vulpiani A 1981 *J. Phys. A* **14** L453
[2] Nicolis C 1982 *Tellus A* **34** 1
[3] Van der Sande G, Verschaffelt G, Danckaert J and Mirasso C R 2005 *Phys. Rev. E* **72** 016113
[4] Duan L, Ren Y and Duan F 2022 *Chaos, Solitons Fractals* **162** 112429
[5] Gabbiani F, Metzner W, Wessel R and Koch C 1996 *Nature* **384** 564
[6] Narins P M 2001 *Nature* **410** 644
[7] Zhang Y, Jin Y and Li Y 2021 *Physica D* **422** 132908
[8] Zhang Y, Jin Y and Xu P 2020 *Int. J. Mech. Sci.* **172** 105418
[9] Duan L, Duan F, Chapeau-Blondeau F and Abbott D 2020 *Phys. Lett. A* **384** 126143
[10] Fu Y, Kang Y and Chen G 2020 *Front. Comput. Neurosci.* **14** 24
[11] Liu X, Duan L, Duan F, Chapeau-Blondeau F and Abbott D 2021 *Phys. Lett. A* **403** 127387
[12] Jin Y, Wang H, Xu P and Xie W 2023 *Probab. Eng. Mech.* **72** 103418
[13] Zhai Y, Fu Y and Kang Y 2023 *IEEE Trans. Instrum. Meas.* **72** 3508011
[14] Murali K, Sinha S, Ditto W L and Bulsara A R 2009 *Phys. Rev. Lett.* **102** 104101
[15] Murali K, Rajamohamed I, Sinha S, Ditto W and Bulsara A 2009 *Appl. Phys. Lett.* **95** 194102
[16] Zhang L, Song A and He J 2010 *Phys. Rev. E* **82** 051106
[17] Xu Y, Jin X and Zhang H 2013 *Phys. Rev. E* **88** 052721
[18] Cheng G, Liu W, Gui R and Yao Y 2020 *Chaos, Solitons Fractals* **131** 109514
[19] Wu J, Xu Y and Ma S 2019 *Chaos, Solitons Fractals* **119** 171
[20] Wang N and Song A 2014 *Eur. Phys. J. B* **87** 117
[21] Dari A, Kia B, Bulsara A and Ditto W 2011 *Chaos* **21** 047521
[22] Dari A, Kia B, Wang X, Bulsara A R and Ditto W 2011 *Phys. Rev. E* **83** 041909

[23] Zhang L, Zheng W, Xie F and Song A 2017 *Phys. Rev. E* **96** 052203
[24] Wang N and Song A 2015 *Neurocomputing* **155** 80
[25] Sharma A, Kohar V, Shrimali M D and Sinha S 2014 *Nonlinear Dyn.* **76** 431
[26] Cheng G, Zheng S, Dong J, Xu Z and Gui R 2021 *Chaos* **31** 053105
[27] Gui R, Li J, Yao Y and Cheng G 2021 *Chaos, Solitons Fractals* **148** 111043
[28] Aravind M, Murali K and Sinha S 2018 *Phys. Lett. A* **382** 1581
[29] Gupta A, Sohane A, Kohar V, Murali K and Sinha S 2011 *Phys. Rev. E* **84** 055201
[30] Yao Y, Cheng G and Gui R 2020 *Chaos* **30** 073125
[31] Huang S, Yang J, Liu H and Sanjuán M 2021 *Int. J. Bifurcation Chaos* **31** 2150246
[32] Storni R, Ando H, Aihara K, Murali K and Sinha S 2012 *Phys. Lett. A* **376** 930
[33] Zhang H, Xu Y, Xu W and Li X 2012 *Chaos* **22** 043130
[34] Zhang H, Yang T, Xu W and Xu Y 2014 *Nonlinear Dyn.* **76** 649
[35] Lu S, Dai Z, Liu Y, Liu G, Yang H and Wang F 2019 *Chin. J. Phys.* **58** 179
[36] Liao Z, Ma K, Shamim Sarker M, Yamahara H, Seki M and Tabata H 2022 *Results Phys.* **42** 105968
[37] Kang Y, Xu J and Xie Y 2003 *Acta Phys. Sin.* **52** 2712 (in Chinese)
[38] Nicolis C and Nicolis G 2017 *Phys. Rev. E* **95** 032219
[39] Lei Y, Bi H and Zhang H 2018 *Chaos* **28** 073104
[40] Bi H, Lei Y and Han Y 2019 *Physica A* **525** 1296
[41] Sancho J M, San Miguel M, Katz S L and Gunton J D 1982 *Phys. Rev. A* **26** 1589
[42] Cao L, Wu D and Ke S 1995 *Phys. Rev. E* **52** 3228
[43] Liang G, Cao L and Wu D 2002 *Phys. Lett. A* **294** 190